JACC: BASIC TO TRANSLATIONAL SCIENCE VOL. 7, NO. 6, 2022


PRECLINICAL RESEARCH

# Cardiac Spinal Afferent Denervation Attenuates Renal Dysfunction in Rats With Cardiorenal Syndrome Type 2

Zhiqiu Xia, MD, PhD,[a] Neetha Nanoth Vellichirammal, PhD,[b] Li Han, PhD,[a,c] Lie Gao, MD, PhD,[d] Erika I. Boesen, PhD,[d] Alicia M. Schiller, PhD,[a] Peter R. Pellegrino, MD, PhD,[a] Steven J. Lisco, MD,[a] Chittibabu Guda, PhD,[b,e] Irving H. Zucker, PhD,[d] Han-Jun Wang, MD[a,d]

## VISUAL ABSTRACT

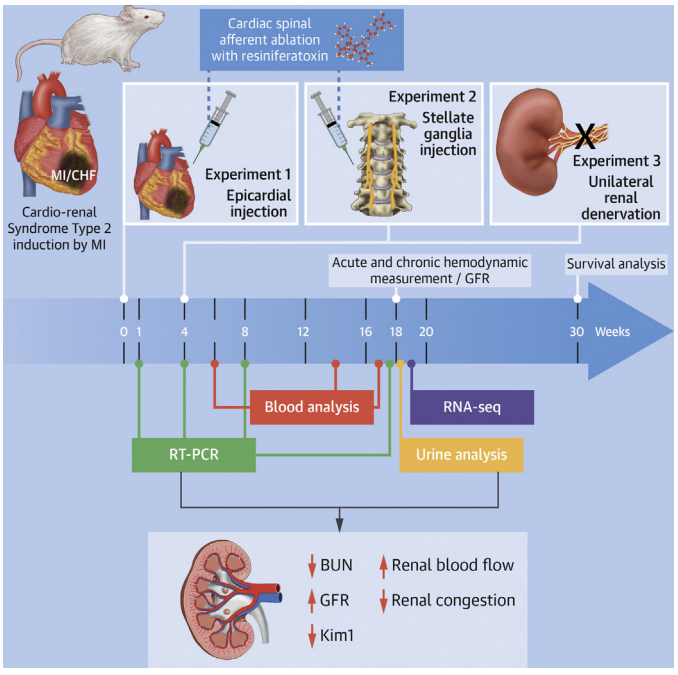


Xia Z, et al. J Am Coll Cardiol Basic Trans Science. 2022;7(6):582-596.

## HIGHLIGHTS

- Epicardial application of RTX at the time of MI largely prevented renal dysfunction, attenuated renal congestion, and partially restored renal blood flow in rats with CHF.
- RNA sequencing analysis showed that renal injury, inflammation, hypoxia, and apoptosis genes were significantly up-regulated in the renal tissue of CHF rats, which was largely prevented by epicardial RTX at the time of MI.
- Cardiac afferent ablation by intra-stellate ganglia injection of RTX or unilateral renal denervation 4 weeks after MI had similar renal protective effects on renal tubular damage in CHF rats.
- These data provide evidence for cardiac spinal afferent modulation of renal function and a potential targeted therapy.

From the [a]Department of Anesthesiology, University of Nebraska Medical Center, Omaha, Nebraska, USA; [b]Department of Genetics, Cell Biology, and Anatomy, University of Nebraska Medical Center, Omaha, Nebraska, USA; [c]College of Veterinary Medicine, Huazhong Agricultural University, Wuhan, China; [d]Department of Cellular and Integrative Physiology, University of Nebraska Medical Center, Omaha, Nebraska, USA; and the [e]Bioinformatics and Systems Biology Core, University of Nebraska Medical Center, Omaha, Nebraska, USA.

The authors attest they are in compliance with human studies committees and animal welfare regulations of the authors' institutions and Food and Drug Administration guidelines, including patient consent where appropriate. For more information, visit the Author Center.

Manuscript received January 7, 2022; revised manuscript received February 15, 2022, accepted February 16, 2022.

ISSN 2452-302X https://doi.org/10.1016/j.jacbts.2022.02.008

## SUMMARY

Cardiorenal syndrome type 2 (CRS2) is defined as a chronic cardiovascular disease, usually chronic heart failure (CHF), resulting in chronic kidney disease. We hypothesized that the cardiac spinal afferent reflex (CSAR) plays a critical role in the development of CRS2. Our data suggest that cardiac afferent ablation by resiniferatoxin not only improves cardiac function but also benefits the kidneys and increases long-term survival in the myocardial infarction model of CHF. We also found that renal denervation has a similar reno-protective effect in CHF rats. We believe this novel work contributes to the development of a unique neuromodulation therapy to treat CHF patients. (J Am Coll Cardiol Basic Trans Science 2022;7:582–596) 

## ABBREVIATIONS AND ACRONYMS

**BUN** = blood urea nitrogen

**CHF** = chronic heart failure

**CRS2** = cardiorenal syndrome type 2

**CSAR** = cardiac spinal afferent reflex

**EF** = ejection fraction

**FS** = fractional shortening

**GFR** = glomerular filtration rate

**HR** = heart rate

**Kim-1** = kidney injury molecule 1

**MAP** = mean arterial blood pressure

**MI** = myocardial infarction

**Ngal** = neutrophil gelatinase-associated lipocalin

**RTX** = resiniferatoxin

**RBF** = renal blood flow

**RVR** = renal vascular resistance

**URDN** = unilateral renal denervation

Chronic heart failure (CHF) is a serious and debilitating disease associated with high morbidity and mortality.[1] About one-half of patients with CHF also exhibit chronic renal dysfunction, prolonging hospitalization with a poor prognosis.[2] Cardiorenal syndromes (CRSs) describe the complex and bidirectional interaction between the heart and kidneys in acute and chronic conditions. CRSs are divided into 5 categories, among which CRS types 1 and 2 involve acute and chronic cardiovascular disease scenarios leading to acute kidney injury or chronic kidney disease.[3] Insufficient renal perfusion due to impaired cardiac function, previously thought to be a primary hemodynamic precipitant in the development of renal dysfunction in CRS types 1 and 2, fails to explain the worsening renal function that is observed clinically.[4] In addition, venous congestion and other major pathophysiologic mechanisms, such as neurohormonal dysregulation, inflammation, and oxidative stress, exert deleterious effects on both the heart and the kidneys.[2] However, the upstream factors that drive these changes in the setting of CHF are not completely understood.

The cardiac spinal afferent reflex (CSAR) is a pathologic sympathoexcitatory reflex which is normally silent but becomes activated in cardiovascular disease, including hypertension, acute myocardial ischemia, and congestive heart failure.[5,6] Previous work from our laboratory confirmed the presence of tonically active cardiac afferent reflexes in rats with CHF that contribute to exaggerated cardiac and renal sympathoexcitation.[5-7] Chemical ablation of cardiac spinal afferents by epicardial application of resiniferatoxin (RTX),[8] an ultrapotent analog of capsaicin that is capable of inducing rapid degeneration of transient receptor potential cation channel subfamily V member 1-expressing afferent neurons and fibers, resulted in the attenuation of exaggerated renal and cardiac sympatho-excitation and amelioration of adverse ventricular remodeling after myocardial infarction.[9] However, whether selective CSAR ablation offers beneficial effects in CRS type 2 (CRS2) is unknown. The primary aim of the present study was to investigate the role of the CSAR in mediating the pathologic development of renal impairment in CRS2.

## METHODS

All animal experimentation was approved by the Institutional Animal Care and Use Committee of the University of Nebraska Medical Center and performed in accordance with the National Institutes of Health's Guide for the Care and Use of Laboratory Animals. The overall experimental protocol is outlined in Supplemental Figure 1. Primer sequences for RT- PCR are listed in Supplemental Table 1. Detailed methods are provided in the Supplemental Appendix.

All data are expressed as mean ± SD and were analyzed with the use of GraphPad Prism 9.0. The Shapiro-Wilk test was used for assessing distribution. The 2-tailed Student *t* test and 1-way analysis of variance (ANOVA) were used for data that were normally distributed, and the Mann-Whitney *U* test and Kruskal-Wallis test were used for data that were not normally distributed. Differences between groups were determined with the use of a 2-way ANOVA followed by Tukey's post hoc test for multiple pairwise comparisons. Survival estimates between vehicle-treated and RTX-treated rats, conditional on survival until the end of week 1 after myocardial infarction (MI), were calculated with the use of Kaplan-Meier methods and compared by means of the log-rank test. A value of $P < 0.05$ was considered to be statistically significant.

## RESULTS

**EVALUATION OF BASELINE HEMODYNAMICS.** Echocardiographic and hemodynamic measurements in all groups are summarized in Supplemental Table 2

**TABLE 1 Blood Analysis in Sham, CHF+Vehicle, and CHF+RTX Rats**

| | Sham (n = 8) | | | CHF+Vehicle (n = 14) | | | CHF+RTX (n = 8) | | |
|---|---|---|---|---|---|---|---|---|---|
| | 6-8 wk | 12-14 wk | 16-18 wk | 6-8 wk | 12-14 wk | 16-18 wk | 6-8 wk | 12-14 wk | 16-18 wk |
| Na, mmol/L | 140.8 ± 1.1 | 140.6 ± 0.9 | 140.9 ± 1.1 | 140.1 ± 1.8 | 138.6 ± 1.8 | 140.7 ± 0.9 | 139.9 ± 1.3 | 137.7 ± 1.4 | 140.8 ± 0.7 |
| K, mmol/L | 4.10 ± 0.19 | 4.03 ± 0.23 | 4.00 ± 0.16 | 4.23 ± 0.28 | 4.14 ± 0.29 | 4.71 ± 0.25[a] | 4.14 ± 0.22 | 4.07 ± 0.16 | 4.19 ± 0.26[b] |
| Cl, mmol/L | 102.3 ± 2.1 | 101.8 ± 2.2 | 102.5 ± 2.5 | 101.5 ± 1.8 | 101.5 ± 1.3 | 102.5 ± 3.1 | 102.1 ± 1.6 | 102.3 ± 1.0 | 101.9 ± 1.5 |
| iCa, mmol/L | 1.23 ± 0.09 | 1.22 ± 0.13 | 1.20 ± 0.07 | 1.31 ± 0.09 | 1.32 ± 0.03 | 1.23 ± 0.06 | 1.21 ± 0.07 | 1.25 ± 0.07 | 1.19 ± 0.05 |
| $TCO_2$, mmol/L | 25.4 ± 4.0 | 25.5 ± 3.8 | 25.9 ± 3.3 | 26.2 ± 1.7 | 26.3 ± 1.6 | 26.1 ± 3.0 | 25.6 ± 2.2 | 26.4 ± 1.8 | 25.4 ± 1.5 |
| BUN, mg/dL | 20.3 ± 1.6 | 21.3 ± 1.3 | 21.6 ± 2.2 | 22.2 ± 2.5 | 22.9 ± 2.6 | 30.9 ± 5.6[a] | 21.8 ± 2.3 | 21.6 ± 1.8 | 25.8 ± 2.8[b] |
| Crea, mg/dL | 0.53 ± 0.14 | 0.54 ± 0.13 | 0.56 ± 0.09 | 0.43 ± 0.22 | 0.47 ± 0.09 | 0.71 ± 0.18[a] | 0.43 ± 0.19 | 0.36 ± 0.12 | 0.55 ± 0.11[b] |
| HCt, %PCV | 48.8 ± 3.2 | 49.3 ± 3.8 | 49.0 ± 3.3 | 46.9 ± 3.1 | 45.7 ± 2.4 | 51.7 ± 6.2 | 46.6 ± 4.2 | 43.7 ± 1.8 | 52.5 ± 1.9 |
| Hb, g/dL | 16.2 ± 1.7 | 16.9 ± 1.2 | 16.7 ± 1.1 | 16.4 ± 0.9 | 15.5 ± 0.8 | 17.5 ± 2.2 | 15.7 ± 0.9 | 14.5 ± 0.4 | 17.9 ± 0.6 |
| AnGap | 17.5 ± 3.9 | 17.8 ± 3.1 | 17.8 ± 3.3 | 16.3 ± 2.4 | 15.9 ± 2.2 | 17.6 ± 2.5 | 13.3 ± 1.9 | 12.7 ± 1.8 | 18.6 ± 1.4 |

Values are mean ± SD. Cardiac spinal afferent reflex ablation by resiniferatoxin prevents the renal dysfunction measured by blood creatinine, BUN, and potassium in rats with chronic heart failure. [a]$P < 0.05$ vs 6-8 wk or 12-14 wk. [b]$P < 0.05$ vs CHF+Vehicle.

AnGap = anion gap; BUN = blood urea nitrogen; Cl = chloride; Crea = creatinine; Hb = hemoglobin; HCt = hematocrit; iCa = ionized calcium; K = potassium; Na = sodium; $TCO_2$ = total carbon dioxide.

for rats that had blood chemistry measurements (i-STAT; Abbott) and Supplemental Table 3 for those rats in which we examined the acute activation of the CSAR. CHF+vehicle rats exhibited increased heart weights, heart weight and lung weight to body weight ratios, and left ventricular end-diastolic pressure compared with sham rats, which were all attenuated by RTX application. CHF+vehicle rats had reduced ejection fraction (EF), fractional shortening (FS), and left ventricular end-systolic pressure (LVESP) compared with sham rats. EF, FS, LVESP, and infarct sizes of CHF+vehicle and CHF+RTX were, however, similar. The infarct sizes of rats with CHF at different time points were similar (1 week after M:, infarct size 46.9% ± 5.2%; 4 weeks after MI: infarct size 45.4% ± 3.8%; 8 weeks after MI: infarct size 43.5% ± 3.8%; 18 weeks after MI: infarct size 44.5% ± 3.4%; CHF+RTX 18 weeks after MI: infarct size 44.2% ± 2.6%).

**CHRONIC CSAR ABLATION WITH RTX PREVENTS RENAL DYSFUNCTION IN RATS WITH CHF.** Blood analysis of creatinine, blood urea nitrogen (BUN), potassium, and other parameters are summarized in Table 1. In CHF+vehicle rats, we did not see any significant differences in BUN, creatinine, or potassium compared with sham rats until 16-18 weeks after MI. Compared with sham, CHF+vehicle rats exhibited decreased urine output and increased urinary osmolality (Figures 1A and 1B). Animals treated with RTX exhibited significantly increased urine output and decreased blood BUN, creatinine, potassium, and urinary osmolality compared with CHF+vehicle rats.

We found that in CHF rats, urinary kidney injury molecule 1 (Kim-1) concentration and 24-hour Kim-1 excretion were markedly increased compared with those of sham rats. Cardiac spinal afferent ablation by RTX significantly decreased urinary Kim-1 concentration and 24-hour Kim-1 excretion in CHF rats (Figure 1C). Compared with sham rats, the average urinary microalbumin concentration and 24-hour microalbumin excretion in CHF+vehicle rats was significantly higher and was normalized in CHF+RTX rats (Figure 1D). Compared with sham rats, the glomerular filtration rate (GFR) of CHF+vehicle rats was significantly reduced at 16-18 weeks after MI, which was improved by epicardial application of RTX (Figure 1E).

Histologic examination showed that compared with sham rats, there were more dilated tubules, more cast-filled tubules, and more necrotic tubules in the kidneys of the rats with CHF, which were all reduced by RTX (Figures 2A and 2B). Masson trichrome analysis demonstrated that there was substantial fibrosis in the cortex and medulla of the CHF rats. However, RTX significantly decreased collagen deposition in the kidneys of the CHF rats (Figures 2C and 2E). In addition, periodic acid-Schiff staining analysis showed that thickening of glomerular basement membranes was observed in CHF rats, which was also attenuated by CSAR ablation (Figure 2D).

**RNA SEQUENCING ANALYSIS IN KIDNEY TISSUES OF RATS WITH CHF TREATED WITH EPICARDIAL VEHICLE OR RTX.** To further investigate the pathophysiologic mechanisms of CRS2 following RTX treatment, RNA sequencing of the whole kidneys was performed in sham, CHF+vehicle, and CHF+RTX rats. In general, the RNA sequencing data showed that gene expressions of *Kim-1* (*Havcr1*), neutrophil gelatinase-associated lipocalin (*Ngal*; *Lcn2*), interleukin-24 (*Il24*), and *Il6* were increased by 30-100-fold in whole-kidney tissues of CHF+vehicle rats compared with sham rats (Supplemental Figure 2). Gene expressions of nephroblastoma overexpressed

**FIGURE 1** **Cardiac Spinal Afferent Reflex Ablation by RTX Prevents Renal Dysfunction**

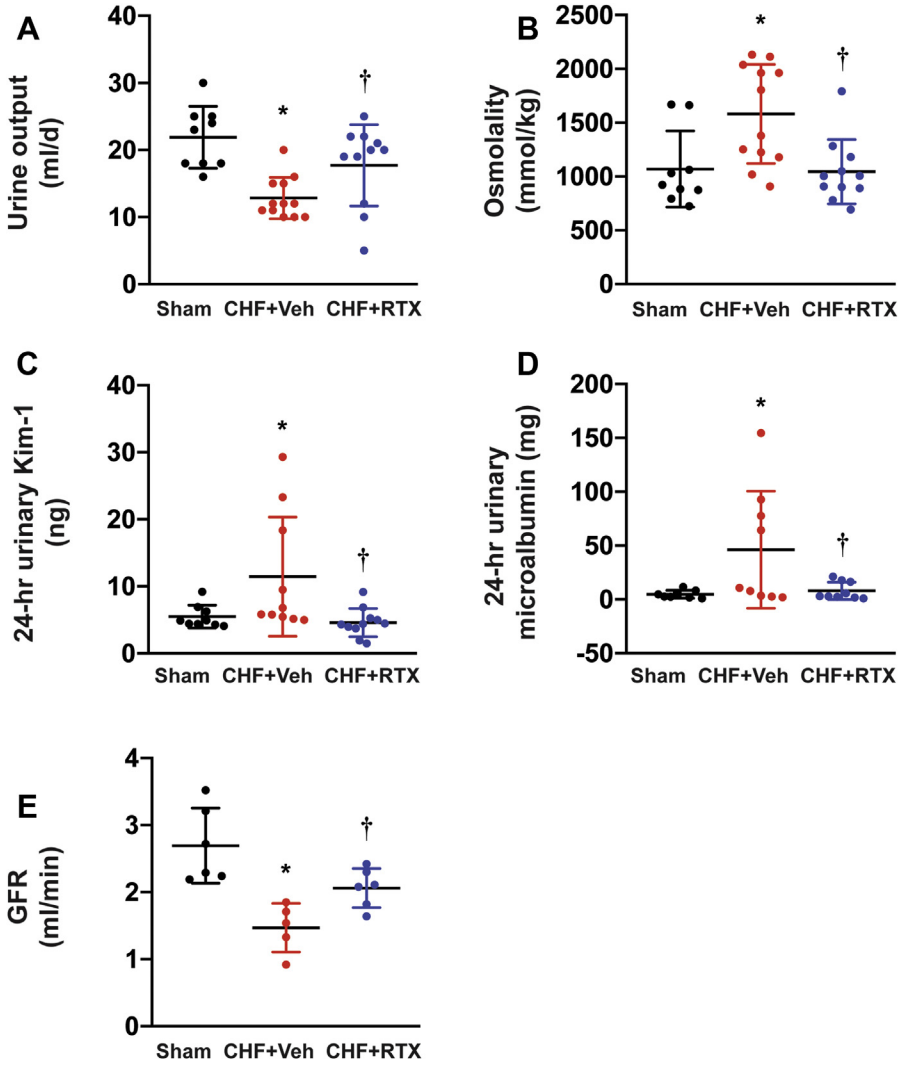


As measured by **(A)** urine output, **(B)** urinary osmolality, **(C)** urinary KIM-1, **(D)** microalbuminuria, and **(E)** GFR in CHF rats. Sham group: n = 9 for **A to C**, n = 8 for **D**, n = 6 for **E**; CHF+Veh group: n = 12 for **A** and **B**, n = 10 for **C**, n = 9 for **D**, n = 5 for **E**; CHF+RTX group: n = 11 for **A to C**, n = 9 for **D**, n = 6 for **E**. **P* < 0.05 vs Sham. †*P* < 0.05 vs CHF+Veh. CHF = chronic heart failure; Kim-1 = kidney injury molecule 1; GFR = glomerular filtration rate; RTX = resiniferatoxin; Veh = vehicle.

(*Nov*), receptor-type tyrosine-protein phosphatase zeta (*Ptprz1*), and hypoxia-inducible factor 3 alpha (*Hif3a*) were increased by 4-7-fold in CHF rats. Significantly enriched Gene Ontology categories for differentially expressed genes including renal injury, inflammation, hypoxia, and apoptosis between sham and CHF+vehicle groups are presented in **Table 2,** Supplemental Figures 3 to 9, and Supplemental Tables 4 and 5.

Comparison of the gene expression profile of CHF+vehicle and CHF+RTX rats revealed an entirely different profile, with the majority of the differentially expressed genes down-regulated in CHF+RTX rats (**Figure 3,** Supplemental Figures 2, 4 and 10 to 12, **Table 2,** Supplemental Table 6). *Kim-1* (*Havcr1*) expression was decreased by ~25-fold in CHF+RTX rats compared with CHF+vehicle rats (**Figure 3C**). However, *Ngal* was similarly elevated in both CHF+vehicle and CHF+RTX rats. Gene expression for *Il24*, *Nov*, and *Ptprzl1* were reduced compared with CHF+vehicle rats. Enriched Gene Ontology categories showed that pathways that regulate Il-1β secretion

**FIGURE 2 Cardiac Spinal Afferent Reflex Ablation by RTX Reduced Renal Fibrosis and Tubular Injury in CHF Rats**

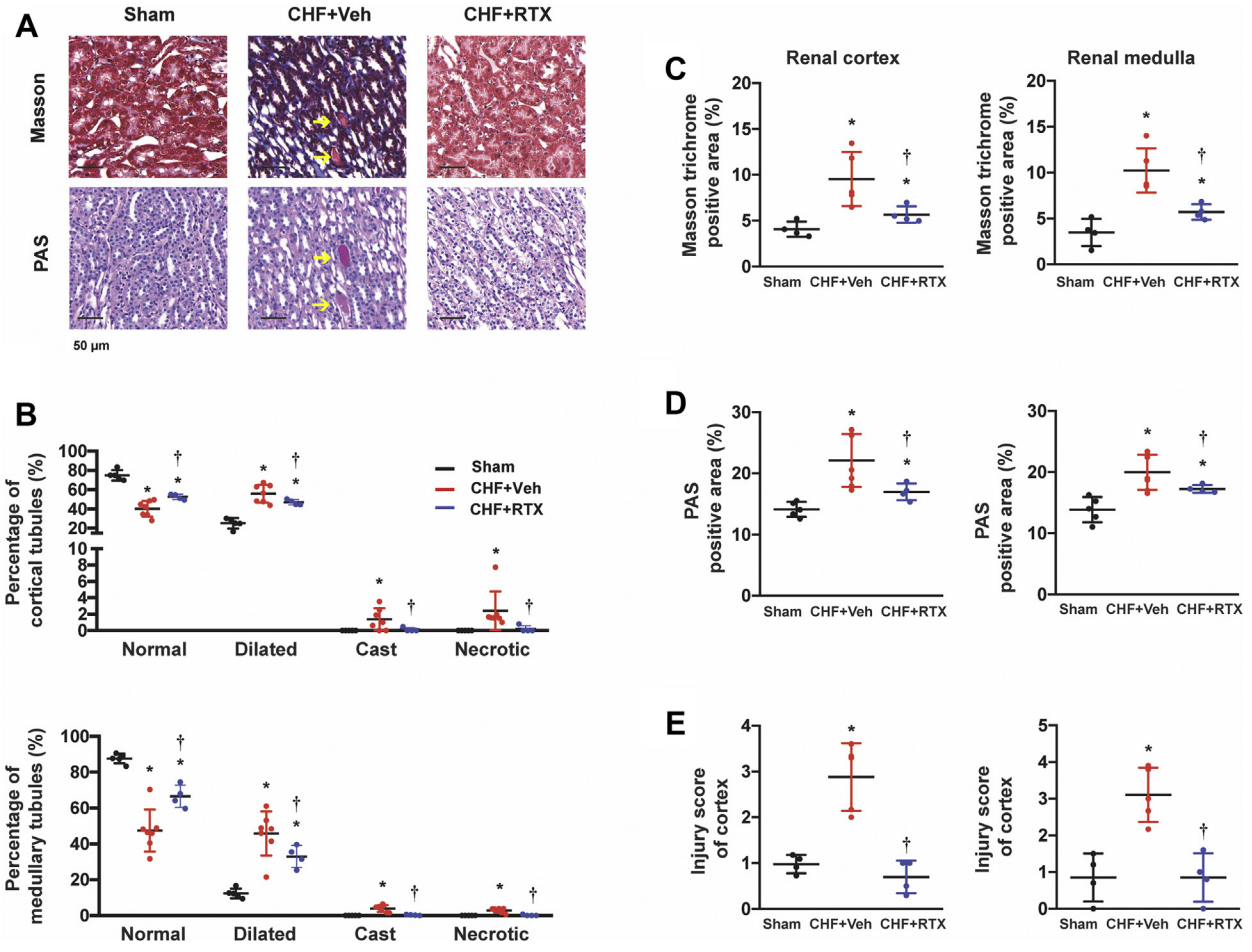


**(A)** Representative images of Masson trichrome staining and PAS staining in the kidneys from Sham, CHF+Veh, and CHF+RTX rats. Scale bar: 50 μm. **Arrows**: cast-filled tubules. **(B)** Percentages of renal tubular profiles categorized as normal, dilated, cast-filled, and necrotic in the cortex and medulla. **(C)** Quantitative analysis for Masson trichrome positive area. **(D)** Quantitative analysis for PAS-positive area. **(E)** Scores of tubular injury. For Masson trichrome staining: Sham group, n = 4; CHF+Veh group, n = 5; CHF+RTX group, n = 4. For PAS staining: Sham group, n = 5; CHF+Veh group, n = 7; CHF+RTX group, n = 4. *$P < 0.05$ vs Sham. †$P < 0.05$ vs CHF+Veh. PAS = periodic acid–Schiff; other abbreviations as in Figure 1.

were enhanced after RTX treatment (Supplemental Figure 5). Ingenuity Pathway Analysis (Qiagen) identified that several pathways involved in Il-12 signaling and production in macrophages, liver X receptor and retinoid X receptor activation, and Wnt/β-catenin signaling were enriched (Supplemental Table 7). More detailed analysis is described in the Supplemental Appendix.

To validate the effects of RTX on mRNA expression of *Kim-1*, subsequent real-time polymerase chain reaction experiments were performed. In the renal cortex of CHF+vehicle rats, *Kim-1* mRNA level was increased by ~300-fold, which was largely prevented in CHF+RTX rats (only 4-fold increase). However, the mRNA expressions of *Ngal* were similar in the renal cortex and medulla of CHF+vehicle rats and CHF+RTX rats compared with sham rats (**Figures 4A to 4D**). mRNA expressions of *Il6* in the renal cortex and medulla were increased in CHF rats regardless of treatment. However, mRNA expression of *Il1b* in the renal cortex was increased by ~4-fold in CHF+vehicle rats, which was attenuated by RTX treatment. In the renal medulla, RTX did not alter mRNA expression of *Il1b* in the CHF+vehicle rats (**Figures 4E to 4H**).

**TIME-COURSE CHANGES OF KIDNEY DAMAGE MARKERS AFTER MI.** To determine the time course of renal damage markers, mRNA expression of *Kim-1* and *Ngal* were measured in the renal cortex and medulla (**Figures 4I to 4L**). We found that both *Kim-1* and *Ngal* levels were increased at 4 weeks after MI,

suggesting the occurrence of acute kidney injury in the early stages after MI. Surprisingly, 8 weeks after MI, *Kim-1* and *Ngal* expression was undetectable. Eighteen weeks after MI, *Kim-1* and *Ngal* expression increased again.

Gene expression of inflammatory cytokines, including *Il1b*, *Il6*, and inducible nitric oxide synthase (*iNos*), was increased during the early stage (1 week and/or 4 weeks) after MI. The expression in rats 8 weeks after MI was similar to that in sham rats, whereas the expression increased again at 4 months after MI (Supplemental Figures 13A to 13D, 13G, and 13H). However, the expression of tumor necrosis factor alpha (*Tnfa*) increased only at 4 weeks after MI (Supplemental Figures 13E and 13F).

Expression of hypoxia-inducible factor 1 alpha (*Hif1a*) and *Hif3a* was increased at 1 month after MI (Supplemental Figures 14C to 14F). However, gene expression of erythropoietin (*Epo*) was increased at the late stage after MI (Supplemental Figures 14A and 14B).

Expression of activating transcription factor 3 (*Atf3*) was increased immediately (1 week) after MI and at the late stage (4 months after MI). Interestingly, gene expression of *Atf3* between 1 week and 8 weeks after MI was normal (Supplemental Figures 15A and 15B).

Gene expression of heme oxygenase 1 (*Hmox1*) was increased at 4 weeks after MI. Similarly, 8 weeks after MI, the expression of *Hmox1* was similar to that in sham rats. However, the expression increased again at 4 months after MI (Supplemental Figures 15C and 15D). In addition, gene expression for arginine vasopressin receptor 2 was decreased at 4 months after MI in CHF+vehicle rats (Supplemental Figures 15E and 15F).

**TABLE 2 Common Differentially Expressed Genes**

| Gene | Fold Difference, CHF+Veh vs Sham | Fold Difference, CHF+RTX vs Sham |
|---|---|---|
| 15 common elements in "Up(sham/CHF+Veh)" and "Dn(CHF+Veh/CHF+RTX)" | | |
| *Havcr1* (*Kim1*) | 104.19 | 4.88 |
| *Il24* | 55.28 | 0.85 |
| *Cyp3a9* | 16.69 | 1.82 |
| *Adra1d* | 9.89 | 1.97 |
| *Gpnmb* | 7.32 | 1.16 |
| *Kng1l1* | 5.98 | 0.95 |
| *Ptprz1* | 5.68 | 1.26 |
| *C4b* | 5.54 | 1.03 |
| *Cd44* | 4.54 | 1.54 |
| *Alox15* | 3.76 | 1.08 |
| *Nov* | 3.61 | 1.07 |
| *Cfi* | 3.48 | 0.87 |
| *Fcrl2* | 3.38 | 1.09 |
| *Ccl19* | 2.77 | 0.67 |
| *Lum* | 2.75 | 0.60 |
| 5 common elements in "Dn(sham/CHF+Veh)" and "Up(CHF+Veh/CHF+RTX)" | | |
| *Slco1a1* | 0.35 | 1.23 |
| *Spata22* | 0.19 | 0.59 |
| *Ptprq* | 0.18 | 1.00 |
| *Ros1* | 0.16 | 0.79 |
| *Cyp2c11l* | 0.07 | 0.75 |
| 3 common elements in "Up(Sham/CHF+Veh)" and "Up(CHF+Veh/CHF+RTX)" | | |
| *Sds* | 7.03 | 37.22 |
| *Pou3f1* | 4.90 | 15.00 |
| *Gnat1* | 4.00 | 11.28 |

CHF = chronic heart failure; Dn = down; RTX = resiniferatoxin; Veh = vehicle.

**ACUTE CSAR ACTIVATION EXAGGERATES RENAL HYPOPERFUSION IN CHF RATS, WHICH IS REDUCED BY RTX.** As shown in Figures 5A to 5E, acute CSAR activation by bradykinin slightly increased mean arterial blood pressure (MAP), heart rate (HR), and renal vascular resistance (RVR) and decreased renal blood flow (RBF) in sham rats. However, compared with sham rats, CHF+vehicle rats exhibited exaggerated increases in MAP, HR, and RVR along with a marked reduction in RBF in response to bradykinin. RVR was significantly increased in the CHF+vehicle rats whereas RBF was significantly decreased compared with sham rats (Figures 5F and 5G). Epicardial RTX application partially restored the abnormal RBF and RVR seen in CHF+vehicle rats.

**CHRONIC CSAR ABLATION WITH RTX ATTENUATES CENTRAL VENOUS PRESSURE IN CHF.** As shown in Figures 6A and 6B, the sham rats displayed typical central venous pressure (CVP), from which we can see a rise in pressure (a-wave) caused by right atrial systole, a decrease in pressure (x-descent) due to right atrial relaxation, a second small peak pressure (v-wave) induced by rapid filling of right atrium, and a second mild decrease of pressure (y-descent) due to atrial emptying. Compared with sham rats, in the setting of CHF the average CVP levels increased, which were ameliorated by CSAR ablation with RTX (Figure 6C).

**CHRONIC CSAR ABLATION WITH RTX IMPROVES SURVIVAL IN RATS WITH CHF.** A subgroup of rats with CHF that were treated with vehicle or RTX were followed for 6 months so that survival could be assessed (Figure 6D). A significant improvement in long-term survival in the RTX-treated CHF group was observed ($P < 0.05$).

**INTRASTELLATE INJECTION OF RTX 4 WEEKS AFTER MI PREVENTS RENAL DYSFUNCTION IN RATS WITH CHF.** To determine if cardiac spinal afferents traverse through

**FIGURE 3 RNA Sequencing Results**

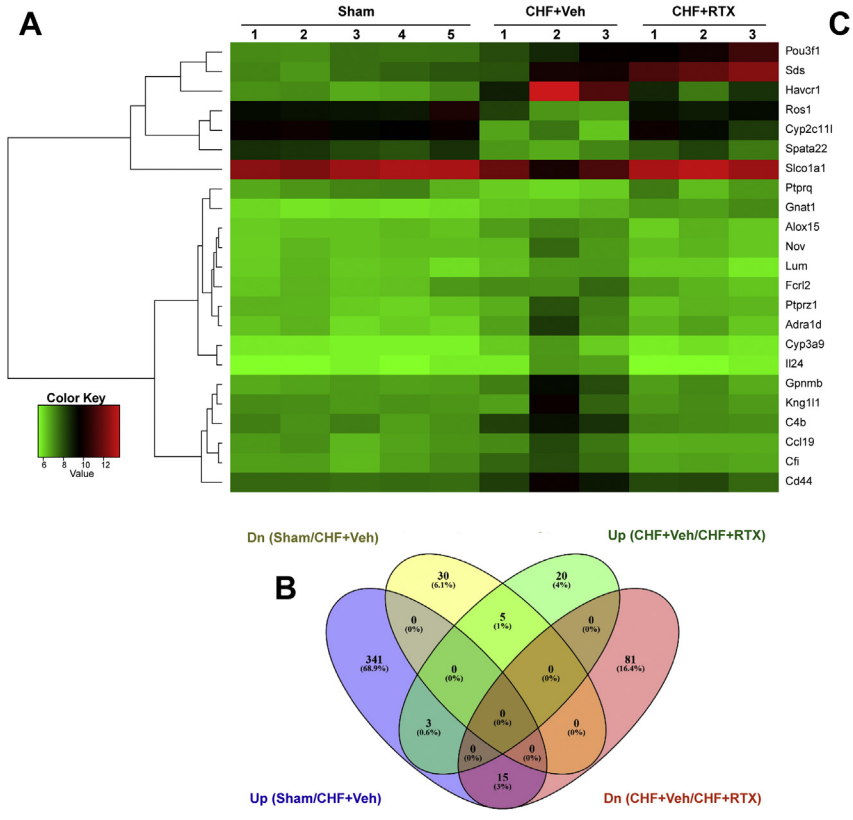


**C**

15 common elements in "Up(Sham/CHF+Veh)" and "Dn(CHF+Veh/CHF+RTX)"

| Genes | Fold (CHF+Veh vs Sham) | Fold (CHF+RTX vs Sham) |
|---|---|---|
| Havcr1 | 104.19 | 4.88 |
| Il24 | 55.28 | 0.85 |
| Cyp3a9 | 16.69 | 1.82 |
| Adra1d | 9.89 | 1.97 |
| Gpnmb | 7.32 | 1.16 |
| Kng1l1 | 5.98 | 0.95 |
| Ptprz1 | 5.68 | 1.26 |
| C4b | 5.54 | 1.03 |
| Cd44 | 4.54 | 1.54 |
| Alox15 | 3.76 | 1.08 |
| Nov | 3.61 | 1.07 |
| Cfi | 3.48 | 0.87 |
| Fcrl2 | 3.38 | 1.09 |
| Ccl19 | 2.77 | 0.67 |
| Lum | 2.75 | 0.6 |

5 common elements in "Dn(Sham/CHF+Veh)" and "Up(CHF+Veh/CHF+RTX)"

| Genes | Fold (CHF+Veh vs Sham) | Fold (CHF+RTX vs Sham) |
|---|---|---|
| Slco1a1 | 0.35 | 1.23 |
| Spata22 | 0.19 | 0.59 |
| Ptprq | 0.18 | 1 |
| Ros1 | 0.16 | 0.79 |
| Cyp2c11l | 0.07 | 0.75 |

3 common elements in "Up(sham/CHF)" and "Up(CHF/CHF-RTX)"

| Genes | Fold (CHF+Veh vs Sham) | Fold (CHF+RTX vs Sham) |
|---|---|---|
| Sds | 7.03 | 37.22 |
| Pou3f1 | 4.9 | 15 |
| Gnat1 | 4 | 11.28 |

**(A)** Heat map of RNA sequencing data showing altered gene profiles in whole-kidney tissues from CHF rats with and without RTX treatment along with sham. Kidney injury molecule 1 (*Kim1*; a specific proximal tubular damage marker) was increased in whole-kidney tissues of CHF rats, which was largely prevented by RTX. **(B)** Venn diagram highlighting the number of genes differentially expressed between CHF/Sham and CHF/CHF-RTX. **(C)** Table showing the common genes changed between different comparisons and the fold change. Sham group: n = 5; CHF+Veh group: n = 3; CHF+RTX group: n = 3. Dn = down; other abbreviations as in Figure 1.

the stellate ganglion (SG), local application of RTX into the SG effectively reduced the CSAR without significant change in cardiac function (Supplemental Figures 16 and 17).

Blood analysis of creatinine, BUN, and electrocytes is summarized in **Table 3**. Compared with SG vehicle, SG RTX reduced BUN.

The mRNA level of *Kim1* in the renal cortex was significantly increased in the CHF+SG vehicle rats but not in the CHF+SG RTX rats compared with sham rats (**Figure 7A**). The mRNA levels of *Ngal* in both renal cortex and medulla were similar between CHF+SG vehicle and CHF+SG RTX rats (**Figures 7C and 7D**). The mRNA expression of *Il6* tended to increase in the kidneys of CHF+SG vehicle and CHF+SG RTX rats (**Figures 7E to 7H**).

**UNILATERAL RENAL DENERVATION (URDN) 4 WEEKS AFTER MI IMPROVES CARDIAC AND RENAL FUNCTION IN RATS WITH CHF.** Unilateral renal denervation reduced the NE and dopamine in the denervated kidneys (Supplemental Figures 18 and 19). Left ventricular dimensions and volumes were increased in a temporal manner after MI, which was not observed in the CHF+URDN rats (Supplemental Figures 20C to 20F). At 18 weeks after MI, the EF and FS of CHF+URDN were significantly improved compared with CHF+sham (Supplemental Figures 20A and 20B).

Compared with control rats, the GFR of CHF+sham denervation rats was significantly reduced at 16 weeks after MI, which was improved in the CHF+URDN group (Supplemental Figure 21). In the renal cortexes from the left and right kidneys of CHF+sham rats, *Kim1* and *Ngal* mRNA levels were significantly increased, which were largely prevented by the unilateral denervation in the left renal cortexes of CHF+URDN rats (**Figures 7I to 7L**). Similar trends were observed in the renal medulla (**Figures 7I to 7L**).

**FIGURE 4** **Effect of Epicardial RTX Application on Renal Injury and Inflammatory Biomarkers Post-Myocardial Infarction**

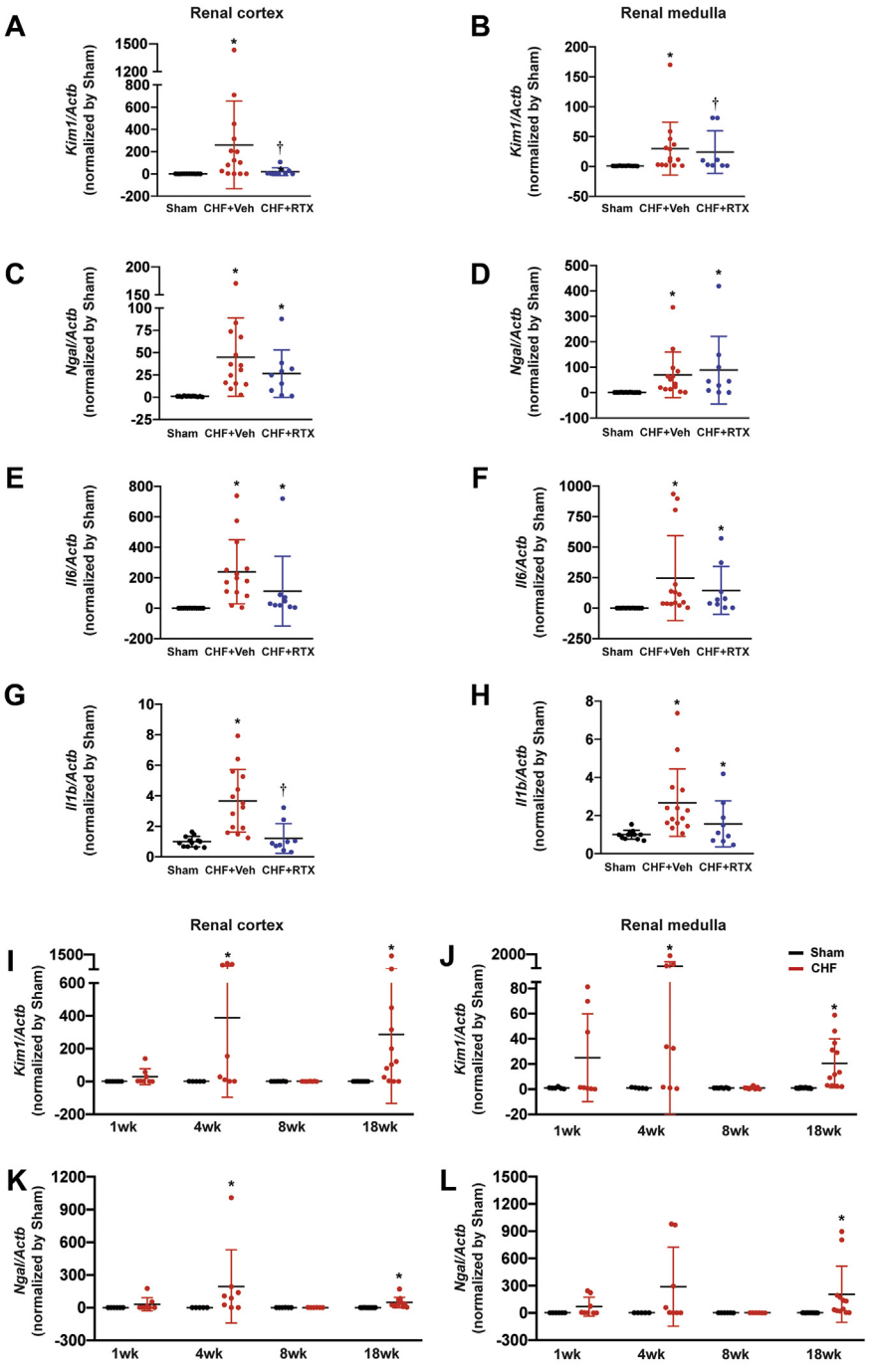


Real-time PCR data showing **(A, B)** *Kim1*, **(C, D)** *Ngal*, **(E, F)** *Il6*, and **(G, H)** *Il1b* mRNA expressions in the renal cortex and medulla from Sham, CHF+Veh, and CHF+RTX rats. Sham group: n = 12 for **A to H**; CHF+Veh group: n = 14 for **A to H**; CHF+RTX group: n = 9 for **A and C to H**, n = 8 for **B**. Real-time PCR data showing the time-course for alterations in **(I, J)** *Kim-1* and **(K, L)** *Ngal* mRNA expressions in renal cortex and medulla from Sham and CHF rats. **(I, J)** For 1 week, 4 weeks, 8 weeks, and 18 weeks, respectively, after surgery: Sham group, n = 6, 5, 7, and 12; CHF group, n = 8, 8, 8, and 12. **(K, L)** For 1 week, 4 weeks, 8 weeks, and 18 weeks, respectively, after surgery: Sham group, n = 6, 5, 6, and 12; CHF group, n = 8, 8, 6, and 12. *$P < 0.05$ vs Sham. †$P < 0.05$ vs CHF+Veh. *Actb* = actin-beta; *Il6* = interleukin-6; *Il1b* = interleukin-1beta; *Kim1* = kidney injury molecule 1; *Ngal* = neutrophil gelatinase-associated lipocalin; PCR = polymerase chain reaction; other abbreviations as in Figure 1.

**FIGURE 5 Hemodynamic Measurements After Acute Cardiac Afferent Activation and Chronic Cardiac Afferent Ablation in Response to Epicardial Application of BK**

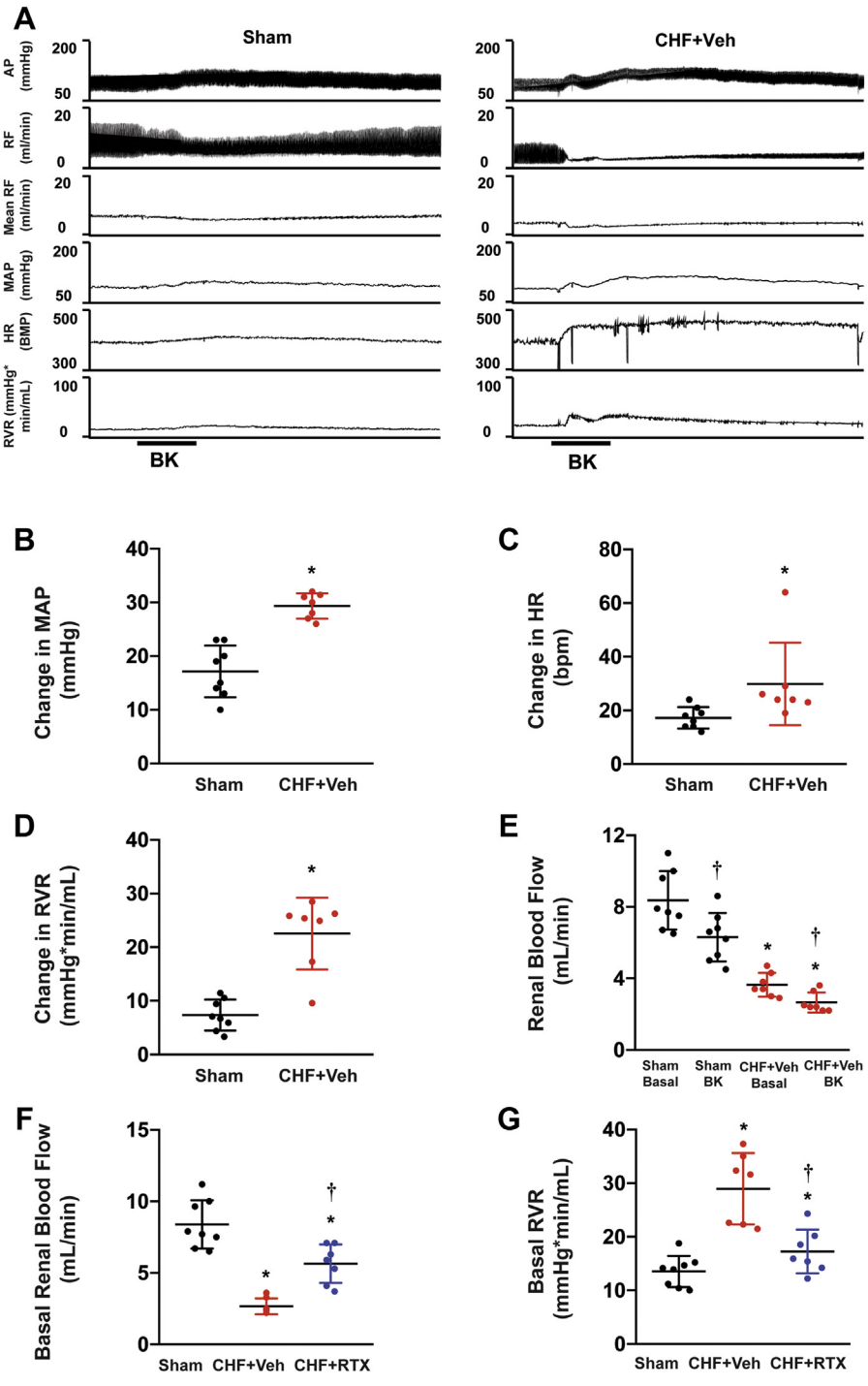


**(A to E)** Cardiac afferent activation caused exaggerated renal vasoconstriction in the post-MI rats. **(F, G)** Cardiac spinal afferent reflex ablation by RTX partially restored the decreased renal blood flow and reduced RVR in CHF rats. Sham group, n = 8; CHF+Veh group, n = 7; CHF+RTX group, n = 7. *$P < 0.05$ vs Sham. †$P < 0.05$ vs CHF+Veh. AP = arterial blood pressure; BK = bradykinin; HR = heart rate; MAP = mean arterial blood pressure; RF = renal blood flow; RVR = renal vascular resistance; other abbreviations as in Figure 1.

**FIGURE 6 CSAR Ablation by RTX Reduced the Increased CVP and Improved Survival in CHF Rats**

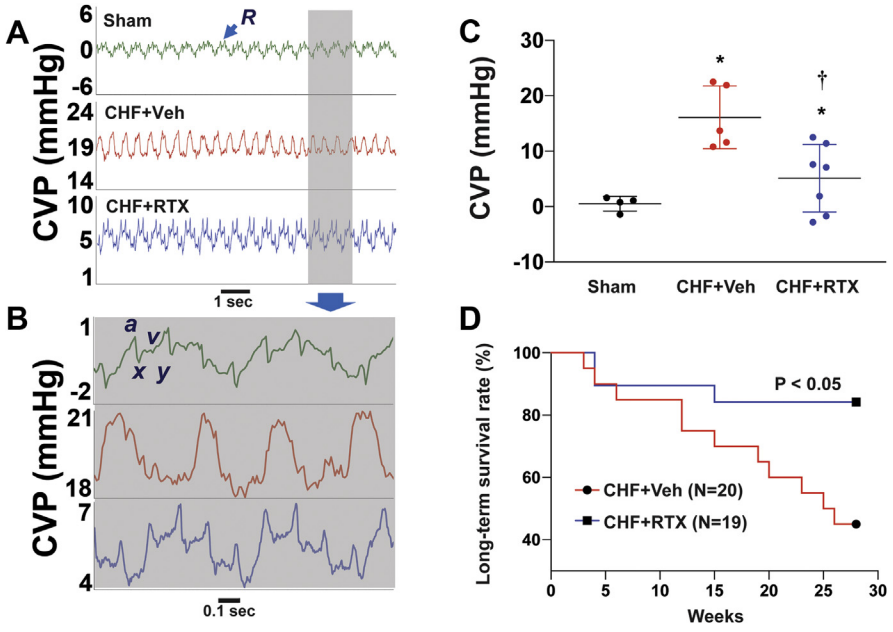


**(A, B)** Original recording and **(C)** summary data showing that cardiac spinal afferent ablation by RTX reduced the increased CVP in CHF rats. R, respiratory wave; a-wave, atrial contraction; x-descent, atrial relaxation; v-wave, systolic filling of atrium; y-descent, early ventricular filling. Sham group, n = 4; CHF+Veh group, n = 5; CHF+RTX group, n = 7. *$P < 0.05$ vs Sham. †$P < 0.05$ vs CHF+Veh. **(D)** Kaplan-Meier survival rates between CHF rats treated with epicardial application of RTX (n = 19) or vehicle (n = 20) at the time of myocardial infarction. CVP = central venous pressure; other abbreviations as in Figure 1.

There was a tendency for the mRNA expression of *Il1b* and *Il6* in the left and right kidneys to increase, which was not attenuated by URDN (Figures 7M to 7P).

## DISCUSSION

Approximately 41% of all-cause mortality in CHF patients is attributed to coexisting renal failure.[10] CRS2 is used to describe renal dysfunction caused by CHF.

**TABLE 3 Blood Analysis in CHF+Sham and CHF+SG RTX Rats**

| | CHF+SG Veh (n = 6) | CHF+SG RTX (n = 6) |
|---|---|---|
| Na, mmol/L | 140.2 ± 0.8 | 140.5 ± 1.4 |
| K, mmol/L | 5.17 ± 1.15 | 4.50 ± 0.62 |
| Cl, mmol/L | 101.3 ± 1.2 | 101.5 ± 1.5 |
| iCa, mmol/L | 1.35 ± 0.09 | 1.35 ± 0.04 |
| $TCO_2$, mmol/L | 29.7 ± 3.3 | 30.3 ± 2.6 |
| BUN, mg/dL | 30.5 ± 5.9 | 23.2 ± 1.7[a] |
| Crea, mg/dL | 0.62 ± 0.19 | 0.43 ± 0.15 |
| HCt, %PCV | 51.2 ± 4.9 | 46.2 ± 1.8 |
| Hb, g/dL | 17.5 ± 1.7 | 15.7 ± 0.6[a] |
| AnGap | 15.2 ± 2.4 | 14.2 ± 1.6 |

Values are mean ± SD. [a]$P < 0.05$ vs CHF+Veh.
SG = stellate ganglion; other abbreviations as in Tables 1 and 2.

However, the mechanism underlying the development of CRS2 remains unclear owing to a lack of an appropriate animal model to mimic this pathologic process. Previously, Lekawanvijit et al[11] found that renal cortical fibrosis and 24-hour urinary albumin increased and were both maximal in rats at 16 weeks after MI. In the present study, we confirmed that at least 16-18 weeks is required for the development of chronic kidney damage in a rat MI model. We also found that the mRNA expression of renal injury genes (*Kim1* and *Ngal*) and proinflammatory genes (*Il1*, *Il6*, *Tnfa*, and *iNos*) in both renal cortex and medulla were higher in MI rats compared with sham at 1, 4, and 18 weeks after MI. However, at 8 weeks after MI, mRNA expression of these genes in MI animals were similar to those of sham, suggesting that there may be a compensatory stage between temporary kidney damage and chronic kidney disease after MI. The advantage of this model is that it resembles the chronic pathologic progression of renal dysfunction in the setting of heart failure that is observed clinically.

Hemodynamic changes due to decreased cardiac output in CHF and dysregulation of neurohumoral systems contribute to the pathophysiology of CRS2.

**FIGURE 7 Real-Time PCR Data**

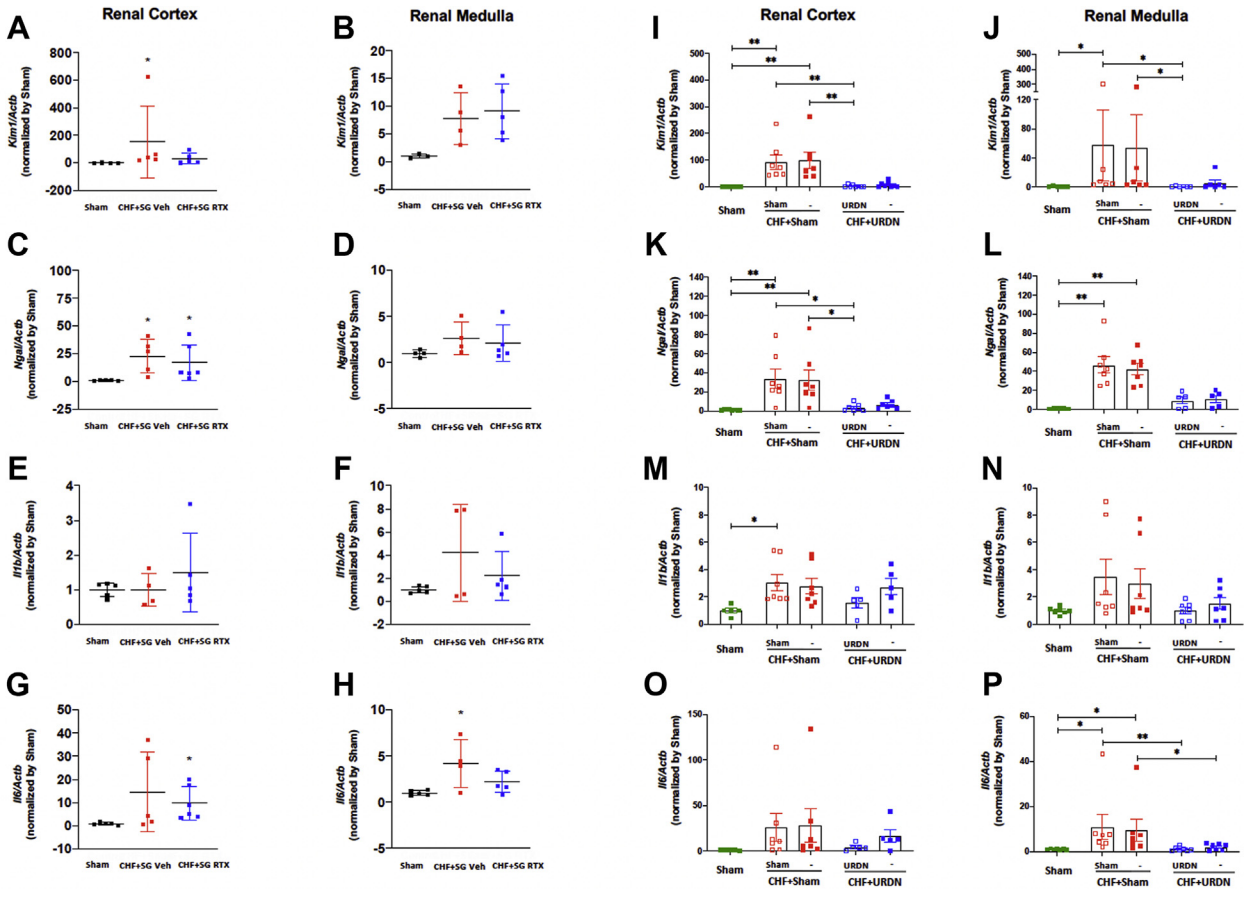


**(A, B)** *Kim1*, **(C, D)** *Ngal*, **(E, F)** *Il1b*, and **(G, H)** *Il6* mRNA expression in the kidneys from Sham, CHF+SG Veh, and CHF+SG RTX rats. **A to H:** Sham group, n = 3-5; CHF+SG Veh group, n = 4-5; CHF+SG RTX group, n = 5-6; *$P < 0.05$ vs Sham. **(I, J)** *Kim1*, **(K, L)** *Ngal*, **(M, N)** *Il1b*, and **(O, P)** *Il6* mRNA expression in kidneys from Sham, CHF+Sham, and CHF+URDN rats. **I to P:** Sham group, n = 5-8; CHF+Sham group, n = 6-7; CHF+URDN group, n = 5-8. *$P < 0.05$. **$P < 0.01$. SG = stellate ganglion; URDN = unilateral renal denervation; other abbreviations as in Figures 1 and 4.

Other factors, such as inflammation, oxidative stress, and metabolic and nutritional changes, also contribute to the pathologic development of renal dysfunction in heart failure.[2] However, the upstream factors that drive these changes are still unclear. In the setting of CHF, one of the most common and significant problems is excessive sympathoexcitation.[12] There are several cardiovascular reflexes contributing to sympathetic excitation including an increased chemoreflex, blunted arterial baroreflex, and enhanced CSAR.[13] The CSAR, a pathologic sympathoexcitatory reflex, is silent in the normal state but becomes tonically activated in CHF and contributes to global sympathoexcitation to the heart and the kidneys.[5,6] We previously provided evidence[9] showing that chronic and selective CSAR ablation by epicardial application of RTX at the time of MI prevented the exaggerated renal and cardiac sympathoexcitation in rats with MI-induced CHF. The present study further demonstrates that epicardial RTX at the time of MI also benefits the kidneys in CHF, as evidenced by improvement in GFR, blood creatinine, BUN, and potassium, and prevention of microalbuminuria by RTX. At the molecular level, we show that epicardial RTX has a selective protective effect on the renal cortex, especially on proximal tubular injury as supported by the reduced mRNA expression of *Kim1* and reduced urinary Kim-1 levels in CHF after RTX application. We also provided additional evidence that CSAR ablation by intrastellate injection of RTX at 4 weeks after MI had a similar renal protective effect, suggesting that CSAR ablation after CHF still exhibits renal beneficial effects. Furthermore, this novel intrastellate RTX injection approach may have more translational

therapeutic potential. Clinically, although epicardial application of RTX is feasible, the MI-induced scar formation and cardiac interstitial fibrosis could affect the efficiency of epicardial RTX on CSAR ablation. Compared with epicardial delivery, injection of RTX into the SG at the post-MI stage may be a better approach to perform CSAR ablation. Anatomically, the stellates not only contain soma for sympathetic efferent fibers but also fibers of passage for thoracic afferents as they course through the dorsal root ganglia and enter the spinal cord. It should be noted that in humans the SG can be easily identified, and that this type of transcutaneous procedure can be performed with the use of fluoroscopic or ultrasound guidance (intraganglionic or nerve "block" approach). Compared with epicardial delivery, which requires relatively larger injection volume (80-100 μL per rat), intrastellate injection requires a much smaller volume (10 μL for bilateral injection), which minimizes the risk of systemic absorption of RTX. Although we did observe similar renal-protective effects between epicardial RTX at the time of MI and SG injection of RTX at 4 weeks after MI, we think that these 2 approaches may still have differential effects due to the intervention time window. Our previous studies suggested that epicardial RTX application at the time of MI largely prevented cardiac remodeling, such as cardiac fibrosis, hypertrophy, and apoptosis, in CHF rats. In rats at 4 weeks after MI, cardiac fibrosis, hypertrophy, and apoptosis have been well developed. We think that cardiac afferent denervation by either epicardial or SG application of RTX at 4 weeks after MI is not capable of reversing the established cardiac remodeling but may prevent or slow the ongoing remodeling process. In other words, the earlier intervention could achieve expanded beneficial effects on both the heart and the kidneys.

Based on our data, it is likely that chronic CSAR ablation improves renal damage by partially restoring RBF in CHF. We confirmed that in the setting of CHF, overactive CSAR modulates renal function through further exacerbation of renal ischemia. CSAR ablation ameliorated the renal vasoconstriction and partially restored RBF, suggesting a protective effect on renal perfusion. Although one could argue that renal autoregulation could counteract the vasoconstrictive effect of CSAR activation, this possibility would be low because autoregulation would simply keep flow constant, whereas CSAR activation caused a long-lasting vasoconstrictor effect in CHF rats.

In the present study, we observed that an increase in CVP in rats with CHF may contribute to renal venous hypertension and loss of renal function, which can be attenuated by RTX. Tonic activation of the CSAR in CHF provides a continuous sympathetically mediated vasoconstrictor tone to visceral vascular beds. The latter, in combination with the decreased intrinsic myocardial contractility, causes a volume shift from the peripheral circulation to the thorax, thus increasing CVP and contributing to renal venous congestion. Based on our hemodynamic data, we propose that both CSAR-induced renal ischemia and venous congestion contribute to chronic kidney dysfunction, which were attenuated by chronic ablation of the CSAR by epicardial RTX.

Our time-course study showed that gene expression of Kim-1 is elevated in the early and late stages after MI, whereas in the intermediate stage, Kim-1 expression was similar to that in sham animals. Tubular expression of Kim-1 is strongly related to interstitial fibrosis and inflammation and negatively associated with renal function.[14] Recently Veach et al showed that human proximal tubule cells responded to various stimuli, including hypoxia (1% $O_2$), indicative of the up-regulation of KIM-1 expression.[15] Renal ischemia plus the reduction in capillary density due to endothelial cell apoptosis after the initial insult may cause renal hypoxia.[16] Our RNA sequencing data show that hypoxia pathways and several hypoxia-related genes, including *Hif1*, *Epo*, and *Ptprz1*, were up-regulated in CHF, suggesting the existence of and the involvement of renal hypoxia in CHF. CSAR ablation attenuated the increased expression of *Ptprz1*, suggesting that the effects of cardiac afferent ablation may reduce hypoxia in CHF. Our RNA sequencing analysis and polymerase chain reaction results also showed that proinflammatory gene expression and inflammatory pathways were up-regulated in the kidneys of CHF rats and were attenuated by CSAR ablation, indicating the involvement of inflammation in the development of renal impairment in CHF. The enhanced sympathetic tone and the activation of RAAS in CHF, which leads to renal vasoconstriction, is considered to be a major cause of local inflammation.[17] In addition, biomechanical stress due to volume overload and venous congestion in CHF promotes the release of proinflammatory mediators from activated vascular endothelium that, in turn, may further impair renal function.[18,19] Venous congestion causes a significant increase in plasma Il-6 and Tnf-α, as well as norepinephrine (NE), in a dog model of CHF.[20] The present study shows that in the renal cortex, the increased gene expression of *Il1b* was attenuated by RTX, which may explain the beneficial effect of CSAR ablation. Overall, chronic CSAR ablation attenuates renal dysfunction by reducing renal ischemia and renal congestion, which may also reduce renal

inflammation. Moreover, apoptosis also contributes to tubular damage and interstitial fibrosis during the progression of chronic kidney damage.[21] In the present study, several genes and pathways related to apoptosis were up-regulated in the setting of CHF, indicating that apoptosis was involved in the pathological process mediating renal damage.

Activation of renal efferent nerves leads to increased RVR and activation of the renin-angiotensin-aldosterone system (RAAS) contributing to sodium and water retention. If CSAR ablation has a beneficial effect on renal function via a renal sympathoexcitatory mechanism in CHF, renal denervation should, at least in part, mimic the beneficial effects of CSAR ablation in CHF rats. In this study, we used a URDN strategy to compare renal injury makers between denervated vs intact kidneys in CHF rats. Surprisingly, we found that URDN significantly reduced gene expressions of *Ngal* and *Kim1* in both denervated and intact kidneys in CHF rats. We also observed that URDN significantly improved cardiac systolic function and reduced cardiac chamber dilation in CHF rats. Previous studies have shown that bilateral RDN prevents the progression of CHF through attenuation of left ventricular fibrosis, reduction in renal sympathetic efferent nerve activity, inhibition of the RAAS, and restoration of impaired natriuresis.[22,23] Our study strongly suggests that URDN is sufficient to improve cardiac dysfunction in CHF rats. Furthermore, this study provided the first data, to our knowledge, suggesting that URDN also improves renal dysfunction in CHF rats. The phenomenon that URDN improves the ipsilateral renal damage in CHF rats could well be explained by a renal efferent nerve-dependent mechanism, which supports our original hypothesis that a decrease in renal sympathetic nerve activity, at least in part, mediates the beneficial effect of CSAR ablation on renal function in CHF rats. However, the beneficial effect of URDN on the contralateral kidney in CHF rats could be explained by renal afferent and/or efferent mechanisms. It is possible that URDN could sufficiently attenuate the RAAS activation via ipsilateral renal efferent nerve, which causes systemic beneficial effects on the heart and the contralateral kidney. Finally, because URDN improved cardiac systolic function in MI rats, it is also possible that URDN has a beneficial effect on the contralateral kidney via its indirect cardioprotective mechanism. Future studies are required to address these questions.

**STUDY LIMITATIONS.** We acknowledge a limitation that only male rats were used in this study. Sex differences in CSAR ablation/URDN-mediated cardioprotective and renoprotective effects in CHF rats remains unclear, and further work will have to be done to determine if such differences exist. Another limitation is that we measured the NE content only in the renal cortex in this study. However, renal NE spillover rather than renal NE content would be more accurate in reflecting renal sympathetic nerve activity,[24] which may explain the similar renal NE content between sham and CHF rats in this study. Nevertheless, renal NE content itself is sufficient to validate the efficacy of RDN, which is a standard and well accepted method used for most RDN studies.[22,25]

## CONCLUSIONS

Both CSAR ablation and URDN have a renoprotective effect in the setting of CHF.

**ACKNOWLEDGMENTS** The authors sincerely thank Dr Kirk W. Foster from the University of Nebraska Medical Center for his help with histologic analysis, Jenifer Phillips from the Medical College of Wisconsin for her help with microalbumin measurements, and Dr Gregory Fink and his high-performance liquid chromatography core laboratory in the Department of Pharmacology and Toxicology, Michigan State University, for measuring tissue NE, dopamine, epinephrine, and serotonin in our renal samples. They also acknowledge the Bioinformatics and Systems Biology Core at the University of Nebraska Medical Center, which receives partial support from National Institutes of Health grants 5P20GM103427 and 5P30CA036727, for providing the infrastructure to conduct data analyses.

## FUNDING SUPPORT AND AUTHOR DISCLOSURES

This study was supported by National Institutes of Health grant 2R01 HL126796, and partially by grants 1R01 HL-152160 and 1R01 HL-121012. Dr Wang is supported by the Margaret R. Larson Professorship in Anesthesiology. Dr Zucker is supported in part by the Theodore F. Hubbard Professorship for Cardiovascular Research. This work was also supported by National Institutes of Health awards 5P20GM103427 and 1P30GM127200 and National Science Foundation Experimental Program to Stimulate Competitive Research award OIA-1557417 to Dr Guda. The authors have reported that they have no relationships relevant to the contents of this paper to disclose.

**ADDRESS FOR CORRESPONDENCE:** Dr Han-Jun Wang, Department of Anesthesiology, University of Nebraska Medical Center, 985850, 42nd and Emile Streets, Omaha, Nebraska 68198, USA. E-mail: hanjunwang@unmc.edu.

## PERSPECTIVES

**COMPETENCY IN MEDICAL KNOWLEDGE:** CHF is a pathologic condition in which the heart is unable to provide sufficient blood flow to meet the needs of the body. CRS2 is used to describe renal dysfunction caused by CHF. However, the mechanism underlying the development of CRS2 remains unclear. We found that in the setting of MI-induced CHF, CSAR-induced sympathetic activation impaired renal function through renal hypoperfusion and potentially through exacerbated renal venous congestion. RTX has been shown to produce analgesic effects in animal models of arthritis and chronic pain when delivered intra-articularly or intrathecally.[26,27] This study suggests that either epicardial or intrastellate application of RTX may have translational potential in the treatment of heart failure patients with CRS. URDN after MI also produced long-term improvements in renal and cardiac function in rats with CHF. This study also suggests a translational potential of URDN in the treatment of heart failure patients.

**TRANSLATIONAL OUTLOOK:** Further large animal and clinical studies are warranted to investigate whether CSAR ablation benefits heart failure patients with CRS2.

## REFERENCES

**1.** Lloyd-Jones D, Adams R, Carnethon M, et al. Heart disease and stroke statistics—2009 update: a report from the American Heart Association Statistics Committee and Stroke Statistics Subcommittee. *Circulation*. 2009;119:e21–181.

**2.** Schefold JC, Filippatos G, Hasenfuss G, Anker SD, von Haehling S. Heart failure and kidney dysfunction: epidemiology, mechanisms and management. *Nat Rev Nephrol*. 2016;12:610–623.

**3.** Ronco C, Haapio M, House AA, Anavekar N, Bellomo R. Cardiorenal syndrome. *J Am Coll Cardiol*. 2008;52:1527–1539.

**4.** Nohria A, Hasselblad V, Stebbins A, et al. Cardiorenal interactions: insights from the ESCAPE trial. *J Am Coll Cardiol*. 2008;51:1268–1274.

**5.** Wang WZ, Gao L, Wang HJ, Zucker IH, Wang W. Interaction between cardiac sympathetic afferent reflex and chemoreflex is mediated by the NTS AT1 receptors in heart failure. *Am J Physiol Heart Circ Physiol*. 2008;295:H1216–h1226.

**6.** Wang HJ, Rozanski GJ, Zucker IH. Cardiac sympathetic afferent reflex control of cardiac function in normal and chronic heart failure states. *J Physiol*. 2017;595:2519–2534.

**7.** Wang WZ, Gao L, Pan YX, Zucker IH, Wang W. AT1 receptors in the nucleus tractus solitarii mediate the interaction between the baroreflex and the cardiac sympathetic afferent reflex in anesthetized rats. *Am J Physiol Regul Integr Comp Physiol*. 2007;292:R1137–1145.

**8.** Zahner MR, Li DP, Chen SR, Pan HL. Cardiac vanilloid receptor 1-expressing afferent nerves and their role in the cardiogenic sympathetic reflex in rats. *J Physiol*. 2003;551:515–523.

**9.** Wang HJ, Wang W, Cornish KG, Rozanski GJ, Zucker IH. Cardiac sympathetic afferent denervation attenuates cardiac remodeling and improves cardiovascular dysfunction in rats with heart failure. *Hypertension*. 2014;64:745–755.

**10.** van Deursen VM, Urso R, Laroche C, et al. Co-morbidities in patients with heart failure: an analysis of the European Heart Failure Pilot Survey. *Eur J Heart Fail*. 2014;16:103–111.

**11.** Lekawanvijit S, Kompa AR, Zhang Y, Wang BH, Kelly DJ, Krum H. Myocardial infarction impairs renal function, induces renal interstitial fibrosis, and increases renal KIM-1 expression: implications for cardiorenal syndrome. *Am J Physiol Heart Circ Physiol*. 2012;302:H1884–H1893.

**12.** Cohn JN, Levine TB, Olivari MT, et al. Plasma norepinephrine as a guide to prognosis in patients with chronic congestive heart failure. *N Engl J Med*. 1984;311:819–823.

**13.** Toschi-Dias E, Rondon M, Cogliati C, Paolocci N, Tobaldini E, Montano N. Contribution of autonomic reflexes to the hyperadrenergic state in heart failure. *Front Neurosci*. 2017;11:162.

**14.** van Timmeren MM, van den Heuvel MC, Bailly V, Bakker SJ, van Goor H, Stegeman CA. Tubular kidney injury molecule-1 (KIM-1) in human renal disease. *J Pathol*. 2007;212:209–217.

**15.** Veach RA, Wilson MH. CRISPR/Cas9 engineering of a KIM-1 reporter human proximal tubule cell line. *PLoS One*. 2018;13:e0204487.

**16.** Ohashi R, Kitamura H, Yamanaka N. Peritubular capillary injury during the progression of experimental glomerulonephritis in rats. *J Am Soc Nephrol*. 2000;11:47–56.

**17.** Ruiz-Ortega M, Ruperez M, Lorenzo O, et al. Angiotensin II regulates the synthesis of proinflammatory cytokines and chemokines in the kidney. *Kidney Int Suppl*. 2002;(82):S12–22.

**18.** Kawai M, Naruse K, Komatsu S, et al. Mechanical stress-dependent secretion of interleukin 6 by endothelial cells after portal vein embolization: clinical and experimental studies. *J Hepatol*. 2002;37:240–246.

**19.** Wang BW, Chang H, Lin S, Kuan P, Shyu KG. Induction of matrix metalloproteinases-14 and -2 by cyclical mechanical stretch is mediated by tumor necrosis factor-alpha in cultured human umbilical vein endothelial cells. *Cardiovasc Res*. 2003;59:460–469.

**20.** Colombo PC, Rastogi S, Onat D, et al. Activation of endothelial cells in conduit veins of dogs with heart failure and veins of normal dogs after vascular stretch by acute volume loading. *J Card Fail*. 2009;15:457–463.

**21.** Docherty NG, O'Sullivan OE, Healy DA, Fitzpatrick JM, Watson RW. Evidence that inhibition of tubular cell apoptosis protects against renal damage and development of fibrosis following ureteric obstruction. *Am J Physiol Renal Physiol*. 2006;290:F4–13.

**22.** Sharp TE 3rd, Polhemus DJ, Li Z, et al. Renal denervation prevents heart failure progression via inhibition of the renin-angiotensin system. *J Am Coll Cardiol*. 2018;72:2609–2621.

**23.** Nozawa T, Igawa A, Fujii N, et al. Effects of long-term renal sympathetic denervation on heart failure after myocardial infarction in rats. *Heart Vessels*. 2002;16:51–56.

**24.** Hasking GJ, Esler MD, Jennings GL, Burton D, Johns JA, Korner PI. Norepinephrine spillover to plasma in patients with congestive heart failure: evidence of increased overall and cardiorenal sympathetic nervous activity. *Circulation*. 1986;73:615–621.

**25.** Xiao L, Kirabo A, Wu J, et al. Renal denervation prevents immune cell activation and renal

inflammation in angiotensin II–induced hypertension. *Circ Res*. 2015;117:547–557.

**26.** Iadarola MJ, Sapio MR, Raithel SJ, Mannes AJ, Brown DC. Long-term pain relief in canine osteoarthritis by a single intra-articular injection of resiniferatoxin, a potent TRPV1 agonist. *Pain*. 2018;159:2105–2114.

**27.** Brown DC, Agnello K, Iadarola MJ. Intrathecal resiniferatoxin in a dog model: efficacy in bone cancer pain. *Pain*. 2015;156:1018–1024.

**KEY WORDS** cardiorenal syndrome type 2, cardiovascular reflexes, chronic heart failure, inflammation, renal failure, sympathoexcitation

**APPENDIX** For supplemental tables, figures, and references, please see the online version of this paper.